STRUCTURE FUNCTIONS OF THE WIND VELOCITY FIELD IN THE ATMOSPHERE FROM THE DATA OF ACOUSTIC SOUNDING

A.Ya. Bogushevich and L.G. Shamanaeva

Institute of Atmospheric Optics,
Siberian Branch of the Russian Academy of Sciences, Tomsk
Received August 28, 1998

The longitudinal structure functions of the wind velocity field for the atmospheric boundary layer are calculated from the Doppler sodar measurements of the vertical profiles of the wind velocity vector. It is demonstrated that the wind velocity field may be highly inhomogeneous in the horizontal plane. The procedure for the acoustic sounding data processing described in the paper is capable of visualization of large-scale inhomogeneities of the wind velocity field in the atmosphere for separation distances up to 3 km.

Acoustic radars (sodars) have found wide application in the study of the dynamic turbulence characteristics in the atmospheric boundary layer. In particular, sodars were used for remote measurements of such parameters, as the temperature (C_T^2) and velocity (C_V^2) structure constants, rate of the turbulent energy dissipation, and outer scale of turbulence (see, for example, Refs. 1–6).

One of the most important characteristics of the random vector field of the atmospheric wind velocity $\mathbf{v}(\mathbf{r})$ is the structural tensor of the second rank[7]

$$D_{ik}(\mathbf{r}, \Delta\mathbf{r}) = <[v_i(\mathbf{r} + \Delta\mathbf{r}) - v_i(\mathbf{r})] \times$$
$$\times [v_k(\mathbf{r} + \Delta\mathbf{r}) - v_k(\mathbf{r})]>,$$

where $\mathbf{r} = \mathbf{r}(x, y, z)$, $\Delta\mathbf{r}$ is the increment of $\mathbf{r}$, $< >$ denotes statistical averaging, and $v_i(\mathbf{r})$ is the projection of the vector $\mathbf{v}(\mathbf{r})$ onto the ith axis of the Cartesian system of coordinates (x, y, z). In general, the tensor $D_{ik}(\mathbf{r}, \Delta\mathbf{r})$ can have up to 9 independent elements. In the theory of atmospheric turbulence the wind velocity field is traditionally considered locally isotropic,[7,8] which reduces the number of independent elements of $D_{ik}(\mathbf{r}, \Delta\mathbf{r})$ to two, named longitudinal, $D_{rr}(\mathbf{r}, \Delta\mathbf{r})$, and transverse, $D_{tt}(\mathbf{r}, \Delta\mathbf{r})$, velocity structure functions. Doppler sodars allow one to record long-term realizations of the instantaneous values of three components of the wind velocity vector. Using these data, the structure functions of the wind velocity field $\mathbf{v}(\mathbf{r})$ in the atmosphere can be calculated and analyzed for separation distances up to several hundreds of meters. In the present paper the longitudinal velocity structure functions $D_{rr}(\mathbf{r})$ are presented for different altitudes above the Earth's surface calculated from the data of sodar measurements of successive series of the vertical profiles of the instantaneous values of the wind velocity vector $\mathbf{v}(z)$.

The vertical profiles of the wind velocity vector were measured with the Zvuk–2 three-channel monostatic Doppler sodar.[9,10] In these measurements, the sodar operating frequency was 1700 Hz, the duration of the sounding pulse was 150 ms, and the pulse repetition period for each channel was $\Delta t = 10.5$ s. The values of the three components of the wind velocity vector were calculated from the Doppler shift of the backscattered signal frequency measured in each of the three channels. One of the transceiving antennas of the sodar was pointed out vertically, and two others were tilted in the orthogonal planes at angles of 20° to the vertical. The instantaneous profiles of the orthogonal components of the wind velocity vector $v_i(z)$ (here, $i = x, y, z$) represented a set of discrete values $v_i(z_k)$ for 24 range gates z_k, 20 m each, from 75 to 535 m. The number of profiles in each run was $N = 53$.

From these data we calculated the temporal longitudinal velocity structure functions $D_{rr}(z_k, n\Delta t)$ for each range gate z_k with a step of Δt. Accepting the hypothesis of frozen turbulence, the spatial structure functions $D_{rr}(z_k, \Delta\mathbf{r})$ were calculated with a step $\Delta t<\mathbf{v}(z_k)>$, where $<\mathbf{v}(z_k)>$ is the wind velocity vector for the range gate z_k averaged over the measurement period $T = N\Delta t$. In so doing, the calculation formula had the form

$$D_{rr}(z_k, n\Delta t <\mathbf{v}(z_k)>) = \frac{1}{N - n - 1} \sum_{j=1}^{N-n-1} [v'_{j+1}(z_k) -$$
$$- v'_j(z_k)]^2, \quad n = 1, 2, ..., N/5,$$

where $j \le N$ is the serial number of the vertical profile of the instantaneous wind vector,

$$|<\mathbf{v}(z_k)>| = \sqrt{<v_x(z_k)>^2 + <v_y(z_k)>^2 + <v_z(z_k)>^2},$$

$$<v_i(z_k)> = \frac{1}{N} \sum_{j=1}^{N} v_{i,j}(z_k) \quad (i = x, y, z),$$

$$v'_j(z_k) = \{v_{x,j}(z_k) <v_x(z_k)> + v_{y,j}(z_k) <v_y(z_k)> +$$
$$+ v_{z,j}(z_k) <v_z(z_k)>\}/|<\mathbf{v}(z_k)>|$$

0235-6880/99/01 53-04 $02.00 © 1999 Institute of Atmospheric Optics

is the instantaneous wind component longitudinal with respect to the direction <**v**(z_k)>. It can easily be noted that the vector of separation between the observation points $\Delta\mathbf{r} = n\Delta t\langle\mathbf{v}(z_k)\rangle$ here practically always is in the horizontal plane, because in the atmosphere the vertical wind component is much less than the horizontal one.

In Figs. 1 – 3(a), the examples of 3-D patterns of the temporal longitudinal velocity structure functions $D_{rr}(z, \Delta t)$ are shown, and in Figs. 1 – 3(b) the corresponding 3-D patterns of the spatial velocity structure functions $D_{rr}(z, \Delta r)$ are shown calculated from the data of acoustic sounding on October 5, 1996 at night from 01:00 till 01:10, on June 25, 1997 in the morning from 10:00 till 10:10, and on July 2, 1997 also in the morning from 10:00 till 10:10, Tomsk local time. The corresponding vertical profiles of the average horizontal wind speed V_h and direction F are shown in Figs. 1 – 3(c, d). These data were chosen by us to illustrate the most interesting types of functions $D_{rr}(z, \Delta\mathbf{r})$ obtained by processing of sodar measurements of the instantaneous wind velocity profiles $\mathbf{v}(z)$.

In all figures the modulus of the horizontal wind velocity component V_h increases with the altitude z from 1.5–2 m/s at the minimum sensing altitude up to 9–14 m/s at altitudes of ~ 300 m. Above 300 m, the modulus of the horizontal wind vector oscillates with the slowing-down tendency to the increase of $V_\text{h}(z)$. In Figs. 1c and d for measurements at night, the wind shear is clearly seen at altitudes of ~ 380 m.

A characteristic feature of the temporal structure functions calculated from the data of acoustic sounding has been revealed, namely, with the increase of the observation time they remain practically constant (at least, they have one order of magnitude), undergoing only local oscillations. At the same time, their magnitudes increase with the sounding altitude z. The similarity of their vertical behavior with that of the horizontal wind velocity component $V_\text{h}(z)$ can be seen.

Figures 1 – 3(b) demonstrate that the longitudinal spatial velocity structure functions $D_{rr}(z, \Delta\mathbf{r})$ can be derived from the data of acoustic sounding for separations between the observation points $\Delta\mathbf{r}$ up to ~ 3000 m. Most typical is the behavior of the spatial velocity structure functions illustrated by Fig. 2b. With the increase of the separation between the observation points $\Delta\mathbf{r}$ they first increase and then saturate. In this case, the greater is the sounding altitude z, the smaller is $\Delta\mathbf{r}$ for which the saturation is observed, owing to larger wind velocities.

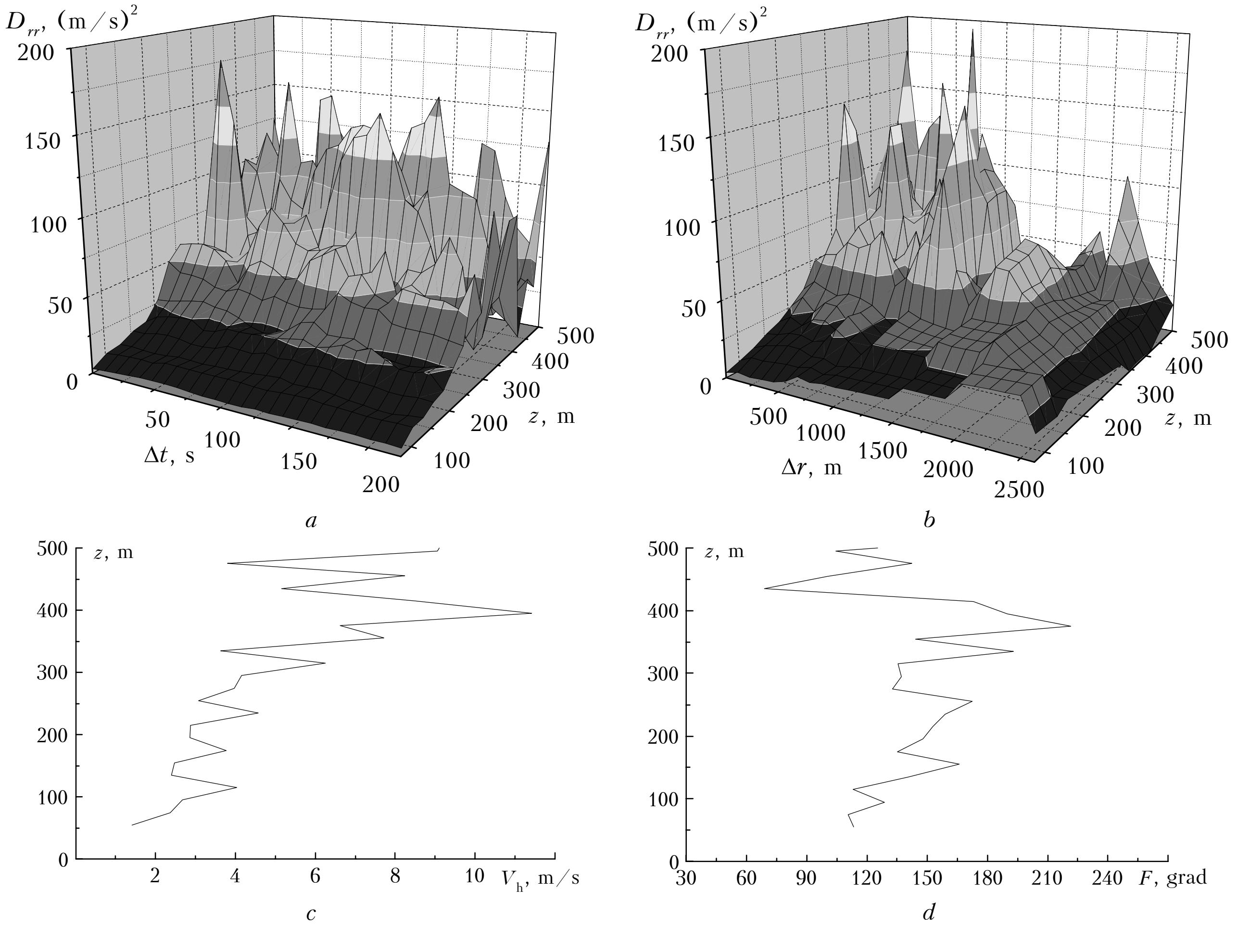

FIG. 1.

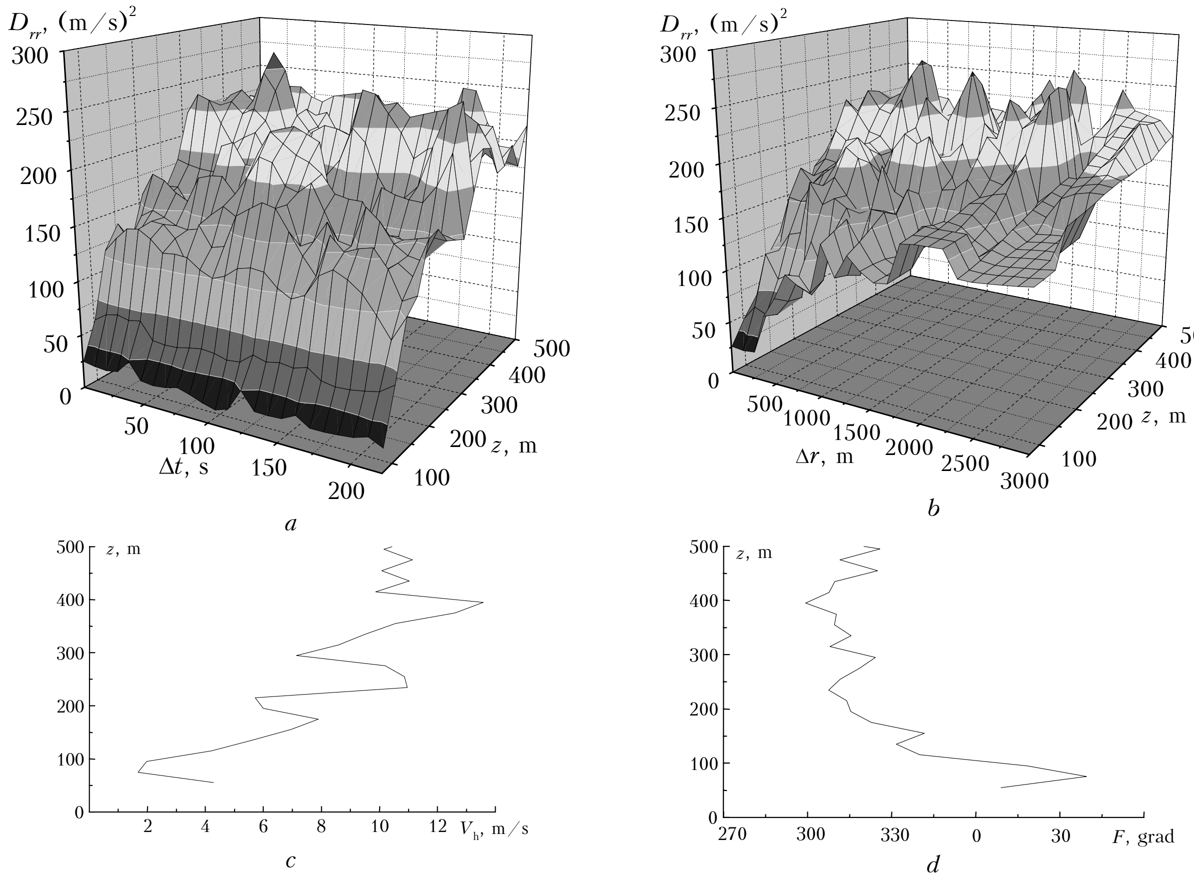

FIG. 2.

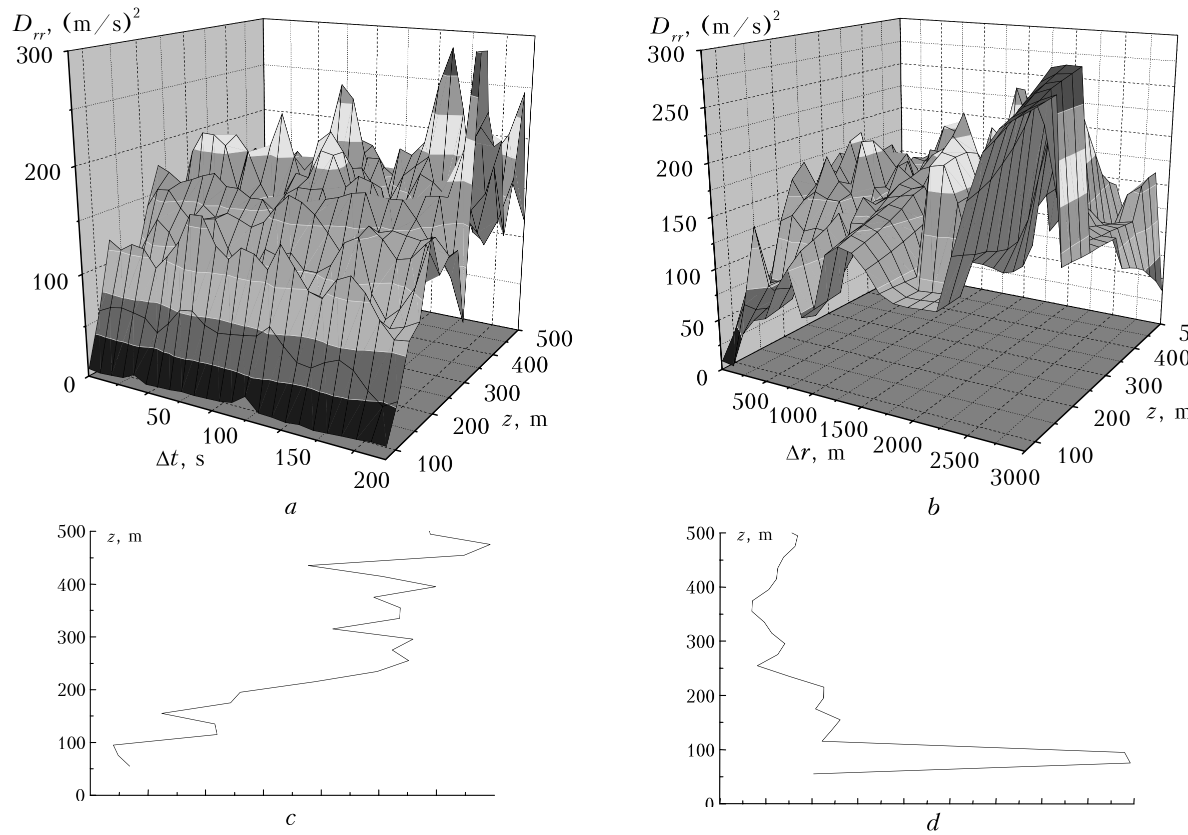

FIG. 3.

An interesting feature has the spatial velocity structure function D_{rr} (z, $\Delta\mathbf{r}$) in the presence of the wind shear (see Fig. 1*b*). Below the wind shear $D_{rr}(z, \Delta\mathbf{r})$ are noticeably suppressed for any separations of the observation points $\Delta\mathbf{r}$, and above the wind shear they sharply increase, but only at relatively small $\Delta\mathbf{r} \le 1000$ m. For the function $D_{rr}(z, \Delta\mathbf{r})$, illustrated by Fig. 3*b*, three maxima are clearly seen for all sensing altitudes and separations between the observation points $\Delta\mathbf{r}$ = 250, 1000, and 1500 m. The position of each maximum on the axis $\Delta\mathbf{r}$ indicates the spatial scale of the strongest inhomogeneities of the wind velocity field $\mathbf{v}(\mathbf{r})$. Such form of the velocity structure function should correspond to a multimodal spatial spectrum of $\mathbf{v}(\mathbf{r})$.

In conclusion, we emphasize that our analysis of the behavior of the longitudinal structure functions of the wind velocity field testifies to its strong spatial inhomogeneity, including inhomogeneity in the horizontal plane. Intermittence regions were observed, in which these functions noticeably differed. The procedure of the acoustic sounding data processing suggested here is capable of spatial visualization of large-scale inhomogeneities of the wind velocity field in the atmospheric boundary layer.

ACKNOWLEDGMENT

The work was supported in part by the Russian Foundation for Basic Researches, Project No. 98–05–03177.

REFERENCES

1. E.H. Brown and F.F. Hall, Rev. Geophys. Space Phys. **16**, No. 1, 47–110 (1978).
2. W.D. Neff, "*Quantitative evaluation of acoustic echoes from the planetary boundary layer*,B Report ERL 322–WPL 38, Boulder, 1975, 34 pp.
3. S.J. Caughey, B.A. Crease, D.N. Asimakopoulos, and R.S. Cole, Quart. J. Roy. Meteorol. Soc. **104**, 147–161 (1978).
4. J.E. Gaynor, J. Appl. Meteorol. **16**, No. 2, 148–155 (1977).
5. N.E. Gerasyuk, M.A. Kallistratova, G.A. Karyukin, et al., Izv. Akad. Nauk SSSR, Fiz. Atmos. Okeana **17**, No. 1, 98–102 (1981).
6. N.P. Krasnenko and L.G. Shamanaeva, Atmos. Oceanic Opt. **11**, No. 1, 60–65 (1998).
7. S.M. Rytov, Yu.A. Kravtsov, and V.I. Tatarskii, *Introduction to Statistical Radio Physics*, (Nauka, Moscow, 1978), P. 2, 463 pp.
8. V.I. Tatarskii, *Wave Propagation in a Turbulent Medium*, (McGraw Hill, New York, 1961).
9. V.A. Gladkikh, V.I. Karpov, N.P. Krasnenko, and V.A. Fedorov, in: *Abstracts of Reports at the third Interrepublic Symposium on Atmospheric and Oceanic Optics*, Tomsk (1996), p. 168.
10. V.A. Gladkikh, N.P. Krasnenko, and V.A. Fedorov, in: *Proceedings of the COST–76 Profiler Workshop*, Vienna (1997), V. 1, pp. 174–177.